Journal of Statistical Physics, Vol. 14, No. 4, 1976

Quantum Statistical Hierarchy Equation in Nonequilibrium Systems

Nobuhiko Mishima,[1] Tomio Yamakoshi Petrosky,[2] and Miwae Yamazaki[3]

Received April 25, 1975

An extension is given for the Fourier expansion method with the contraction technique, which was introduced by Balescu for quantum statistical systems. This is attained by introducing a diagrammatic method with a concept of moving contraction. Then the hierarchy equation for the contracted Fourier coefficient of the Wigner distribution function is obtained. As an application, a generalized master equation involving n-body collision effects and quantum statistical effects is also derived.

KEY WORDS: Wigner distribution function; Fourier expansion method; quantum statistical hierarchy equation; diagrammatic method; movable and unmovable contractions.

1. INTRODUCTION

The purpose of this paper is to give an extension of the Fourier expansion method in nonequilibrium statistical physics, which has been developed by Prigogine and Balescu[(1)] for classical systems and by Balescu[(2)] for quantum statistical systems.

[1] Department of Physics, Tokyo Gakugei University, Koganei-shi, Tokyo, Japan.
[2] Department of Physics, Science University of Tokyo, Kagurazaka, Shinjuku-ku, Tokyo, Japan.
[3] Department of Physics, Saitama University, Urawa-shi, Saitama, Japan.

In treating the long-time behavior of nonequilibrium systems by perturbation theory, the terms corresponding to the diagonal transition play essential roles because of their growing contributions with time.[1-3] In these diagonal transitions, there exists a peculiar transition originating from the quantum statistics. We must, therefore, build up our quantum statistical theory so as to take these effects explicitly into account in the Fourier expansion method. This problem was first discussed by Balescu[2] under the concept of "contraction" in the Fourier coefficients of the Wigner distribution function, and he has tried to get a basic quantum statistical hierarchy equation for these Fourier coefficients. However, in his arguments to derive the hierarchy equation there are inconsistencies and his results are unsatisfactory.

The aim of this paper is to accomplish what Balescu has tried and to give the basic hierarchy equation in the proper form. In this equation the quantum statistical effects are incorporated as effective vertices, and by this equation the diagonal transition originating from the quantum statistics can be treated directly in the perturbation theory. We will derive this equation by introducing a diagrammatic method with a concept of the moving contraction. Details of the method are given in Section 2 and the appendix. Section 3 is devoted to an application of our basic hierarchy equation. There we derive a generalized master equation of the momentum distribution function involving up to n-body collision and any order of the quantum statistical effects.

Here we explain briefly the basic formalism for our problem. We consider a system of N identical particles which obeys the quantum statistics and is enclosed in a box of volume $(2\pi)^3\Omega$ with the usual periodic boundary conditions. The Hamiltonian of the system is assumed to be a sum of single-particle energies and of the pair potentials,

$$H = \sum_{j}^{N} \frac{\boldsymbol{P}_j}{2m} + \sum_{j<n}^{N} V(|\boldsymbol{r}_j - \boldsymbol{r}_n|) \tag{1}$$

where m is the mass of a particle, and $\boldsymbol{P}_j$ and $\boldsymbol{r}_j$ are the momentum and position operators of particle j, respectively.

The density matrix describing the system is defined by the momentum representation as

$$\rho^{(N)}(\boldsymbol{P}_1,..., \boldsymbol{P}_N; \boldsymbol{P}_1',..., \boldsymbol{P}_N'; t) = \sum_i w_i \Psi_i(\boldsymbol{P}_1,..., \boldsymbol{P}_N; t)\Psi_i^*(\boldsymbol{P}_1',..., \boldsymbol{P}_N'; t) \tag{2}$$

where $\Psi_i(\boldsymbol{P}_1,..., \boldsymbol{P}_N; t)$ is the symmetrized or antisymmetrized wave function for the state of the Hamiltonian (1), and w_i is the statistical weight of the

ith state of an ensemble.[4] The time evolution of the density matrix is governed by the well-known von Neumann equation, i.e.,

$$\begin{aligned}\frac{\partial}{\partial t}\rho^{(N)}(\boldsymbol{P}_1,\ldots,\boldsymbol{P}_N;\boldsymbol{P}_1',\ldots,\boldsymbol{P}_N';t)&\\ =\frac{i}{\hbar}\sum_j^N\left(\frac{\boldsymbol{P}_j'^2}{2m}-\frac{\boldsymbol{P}_j^2}{2m}\right)\rho^{(N)}(\boldsymbol{P}_1,\ldots,\boldsymbol{P}_N;\boldsymbol{P}_1',\ldots,\boldsymbol{P}_N';t)&\\ +\frac{i}{\hbar}\sum_{j<n}^N\Omega^{-1}\sum_l\{v(l)\rho^N(\boldsymbol{P}_1,\ldots,\boldsymbol{P}_j,\ldots,\boldsymbol{P}_n,\ldots,\boldsymbol{P}_N;&\\ \boldsymbol{P}_1',\ldots,\boldsymbol{P}_j'-\hbar\boldsymbol{l},\ldots,\boldsymbol{P}_n'+\hbar\boldsymbol{l},\ldots,\boldsymbol{P}_N';t)&\\ -v(l)\rho^{(N)}(\boldsymbol{P}_1,\ldots,\boldsymbol{P}_j+\hbar\boldsymbol{l},\ldots,\boldsymbol{P}_n-\hbar\boldsymbol{l},\ldots,\boldsymbol{P}_N;&\\ \boldsymbol{P}_1',\ldots,\boldsymbol{P}_j',\ldots,\boldsymbol{P}_n',\ldots,\boldsymbol{P}_N';t)\}&\end{aligned}\tag{3}$$

where $v(l)$ is the Fourier transform of $V(r)$,

$$v(l)=[1/(2\pi)^3]\int d\boldsymbol{r}\,V(r)\exp[i\boldsymbol{l}\boldsymbol{r}]\tag{4}$$

In order to give a unified description for both the classical and quantum systems, we introduce the normalized Wigner distribution function,[5] which is defined by

$$\begin{aligned}f_N^{\mathrm{w}}(x,p;t)&\\ =(8\pi^3\Omega)^{-N}\sum_{k_1}\cdots\sum_{k_N}\exp\left[i\sum_i^N\boldsymbol{k}_i\boldsymbol{x}_i\right]&\\ \times\rho^{(N)}\left(\boldsymbol{p}_1+\frac{\hbar}{2}\boldsymbol{k}_1,\ldots,\boldsymbol{p}_N+\frac{\hbar}{2}\boldsymbol{k}_N;\boldsymbol{p}_1-\frac{\hbar}{2}\boldsymbol{k}_1,\ldots,\boldsymbol{p}_N-\frac{\hbar}{2}\boldsymbol{k}_N;t\right)&\end{aligned}\tag{5}$$

where $x\equiv\{\boldsymbol{x}_1,\ldots,\boldsymbol{x}_N\}$ and $p\equiv\{\boldsymbol{p}_1,\ldots,\boldsymbol{p}_N\}$ are defined as whole sets of variables in the quantum phase space of the N-particle system. From (3) and (5) it follows that f_N^{w} satisfies the quantum Liouville equation, i.e.,

$$\begin{aligned}\frac{\partial}{\partial t}f_N^{\mathrm{w}}+\sum_j^N\frac{\boldsymbol{p}_j}{m}\frac{\partial}{\partial\boldsymbol{x}_j}f_N^{\mathrm{w}}-\frac{i}{\hbar}\sum_{j<n}^N\left\{V\left(\left|\boldsymbol{x}_j+\frac{\hbar}{2i}\frac{\partial}{\partial\boldsymbol{p}_j}-\boldsymbol{x}_n-\frac{\hbar}{2i}\frac{\partial}{\partial\boldsymbol{p}_n}\right|\right)\right.&\\ \left.-V\left(\left|\boldsymbol{x}_j-\frac{\hbar}{2i}\frac{\partial}{\partial\boldsymbol{p}_j}-\boldsymbol{x}_n+\frac{\hbar}{2i}\frac{\partial}{\partial\boldsymbol{p}_n}\right|\right)\right\}f_N^{\mathrm{w}}=0&\end{aligned}\tag{6}$$

The reduced distribution functions for a set of s particles are defined as usual[1] in the limit of $\Omega\to\infty$ by

$$\begin{aligned}f_s^{\mathrm{w}}(\boldsymbol{x}_1,\ldots,\boldsymbol{x}_s;\boldsymbol{p}_1,\ldots,\boldsymbol{p}_s;t)&=\frac{N!}{(N-s)!}\int(dx)^{N-s}\int(dp)^{N-s}f_N^{\mathrm{w}}\\ \phi_s(\boldsymbol{p}_1,\ldots,\boldsymbol{p}_s;t)&=\int(dx)^N\int(dp)^{N-s}f_N^{\mathrm{w}}\\ n_s(\boldsymbol{x}_1,\ldots,\boldsymbol{x}_s;t)&=\frac{N!}{(N-s)!}\int(dx)^{N-s}\int(dp)^N f_N^{\mathrm{w}}\end{aligned}\tag{7}$$

According to the Fourier expansion method of Prigogine and Balescu,[1] we introduce the Fourier coefficient $\rho_{k_1,\ldots,k_r}(\boldsymbol{p}_1,\ldots,\boldsymbol{p}_r|\boldsymbol{p}_{r+1},\ldots,\boldsymbol{p}_N;t)$ of the Wigner distribution function in the following form:

$$
\begin{aligned}
f_N^{\mathrm{W}}(x,p;t) = (8\pi^3\Omega)^{-N}\Bigg\{ & \rho_0(|\ldots;t) \\
& + \Omega^{-1}\sum_{j}^{N}\sum_{\boldsymbol{k}_j}{}' \rho_{\boldsymbol{k}_j}(\boldsymbol{p}_j|\ldots;t)\exp\left[i\boldsymbol{k}_j\left(\boldsymbol{x}_j-\frac{\boldsymbol{p}_j}{m}t\right)\right] \\
& + \Omega^{-2}\sum_{i<j}^{N}\sum_{\substack{\boldsymbol{k}_i \\ \boldsymbol{k}_i+\boldsymbol{k}_j\neq 0}}{}'\sum_{\boldsymbol{k}_j}{}' \rho_{\boldsymbol{k}_i,\boldsymbol{k}_j}(\boldsymbol{p}_i,\boldsymbol{p}_j|\ldots;t) \\
& \times \exp\left[i\boldsymbol{k}_i\left(\boldsymbol{x}_i-\frac{\boldsymbol{p}_i}{m}t\right)+i\boldsymbol{k}_j\left(\boldsymbol{x}_j-\frac{\boldsymbol{p}_j}{m}t\right)\right] \\
& + \Omega^{-1}\sum_{i<j}^{N}\sum_{\boldsymbol{k}}{}' \rho_{\boldsymbol{k},-\boldsymbol{k}}(\boldsymbol{p}_i,\boldsymbol{p}_j|\ldots;t) \\
& \times \exp\left[i\boldsymbol{k}\left\{(\boldsymbol{x}_i-\boldsymbol{x}_j)-\frac{(\boldsymbol{p}_i-\boldsymbol{p}_j)}{m}t\right\}\right]+\ldots\Bigg\}
\end{aligned}
\tag{8}
$$

where the prime over a summation sign indicates the exclusion of $\boldsymbol{k}=0$. By comparing this expansion with (5), we get the relation between the Fourier coefficient and the density matrix as

$$
\begin{aligned}
& \rho_{k_1,\ldots,k_r}(\boldsymbol{p}_1,\ldots,\boldsymbol{p}_r|\boldsymbol{p}_{r+1},\ldots,\boldsymbol{p}_N;t)\exp\left[-i\sum_{j}^{r}\boldsymbol{k}_j\boldsymbol{p}_j\frac{t}{m}\right] \\
& \quad = \Omega^{\nu}\rho^{(N)}\left(\boldsymbol{p}_1+\frac{\hbar}{2}\boldsymbol{k}_1,\ldots,\boldsymbol{p}_r+\frac{\hbar}{2}\boldsymbol{k}_r,\boldsymbol{p}_{r+1},\ldots,\boldsymbol{p}_N;\right. \\
& \quad\quad \left.\boldsymbol{p}_1-\frac{\hbar}{2}\boldsymbol{k}_1,\ldots,\boldsymbol{p}_r-\frac{\hbar}{2}\boldsymbol{k}_r,\boldsymbol{p}_{r+1},\ldots,\boldsymbol{p}_N;t\right)
\end{aligned}
\tag{9}
$$

where ν is the number of independent wave vectors in $\boldsymbol{k}_1,\ldots,\boldsymbol{k}_r$. The momentum arguments on the left-hand side of the bar in $\rho_{k_1,\ldots,k_r}$ indicate those of the particles having nonzero wave vectors. The arguments on the right-hand side of the bar [we indicate them by dots in (8)] indicate those of the particles having zero wave vectors. The propagator $\exp[-i\boldsymbol{k}(\boldsymbol{p}/m)t]$ is introduced to treat the von Neumann equation (3) in the interaction representation. In the Fourier coefficient, the nonzero wave vector $\boldsymbol{k}_j$ pertains to the coordinate $\boldsymbol{x}_j$ in the Wigner distribution function and is related to the spatial correlation of the particles. Under the assumption that the coefficients $\rho_{k_1,\ldots,k_r}$ do not depend explicitly on N or Ω, the expansion (8) ensures a regular behavior of the reduced functions (7) in the thermodynamic limit, i.e., $N\to\infty$ and $\Omega\to\infty$ with finite number density, $c\equiv N/8\pi^3\Omega=\text{const.}$

From (3) and (9), and by the use of the displacement operator

$\exp(\hbar \boldsymbol{k}\, \partial/\partial \boldsymbol{p})$ [which means $\exp(\hbar \boldsymbol{k}\, \partial/\partial \boldsymbol{p}) F(\boldsymbol{p}) = F(\boldsymbol{p} + \hbar \boldsymbol{k})$, where $F(\boldsymbol{p})$ is an arbitrary function], it follows that $\rho_{k_1,\ldots,k_r}$ satisfies the hierarchy equation,

$$\begin{aligned}\frac{\partial}{\partial t}\rho_{\{k\}}(p;t) = \frac{i}{\hbar}\Omega^{-1}\sum_{j<n}^{N}\sum_{l}\exp\left[i\left(\boldsymbol{k}_1\frac{\boldsymbol{p}_1}{m}+\ldots+\boldsymbol{k}_r\frac{\boldsymbol{p}_r}{m}\right)t\right] \\ \times\left\{v(l)\exp\left[-\frac{\hbar}{2}\boldsymbol{l}\boldsymbol{D}_{jn}^{(+)}\right]-v(l)\exp\left[-\frac{\hbar}{2}\boldsymbol{l}\boldsymbol{D}_{jn}^{(-)}\right]\right\} \\ \times\exp\left[-i\left(\boldsymbol{k}_1\frac{\boldsymbol{p}_1}{m}+\ldots+(\boldsymbol{k}_j+\boldsymbol{l})\frac{\boldsymbol{p}_j}{m}+\ldots+(\boldsymbol{k}_n-\boldsymbol{l})\frac{\boldsymbol{p}_n}{m}\right.\right. \\ \left.\left.+\ldots+\boldsymbol{k}_r\frac{\boldsymbol{p}_r}{m}\right)t\right]\Omega^{\nu-\nu'}\rho_{k_j+l,k_n-l,\{k\}'}(p;t) \qquad (10)\end{aligned}$$

where

$$\boldsymbol{D}_{jn}^{(\pm)} = \pm\boldsymbol{D}_{jn}, \qquad \boldsymbol{D}_{jn} \equiv \partial/\partial \boldsymbol{p}_j - \partial/\partial \boldsymbol{p}_n \qquad (11)$$

The notation $\{\boldsymbol{k}\}$ is used as an abbreviation for the set $\boldsymbol{k}_1,\ldots,\boldsymbol{k}_r$, and $\{\boldsymbol{k}\}'$ is used for the same set with the exclusion of $\boldsymbol{k}_j$ and $\boldsymbol{k}_n$. The exponents ν and ν' are the numbers of independent wave vectors in ρ on the right- and left-hand sides, respectively. The formal solution of (10), which is referred to as the "iterated solution" or the "iterated expansion" in the following sections, is obtained by iterations of a set of the equivalent integral equations with the appropriate initial conditions at $t = 0$.

We remark here that Eq. (10) has the same form as the equation for the quantum system of distinguishable particle[6] and the quantum statistical effects are contained in $\rho_{\{k\}}(p;t)$. In obtaining the solution of (10), if no special consideration is paid to the contribution of the diagonal transitions originating in the quantum statistical effects, these contributions may be overlooked. Thus it is very useful to reformulate this equation so that these effects are taken explicitly from $\rho_{\{k\}}(\boldsymbol{p};t)$ in the form of effective interactions. In the next section, we will give a method to derive the quantum statistical hierarchy equation.

2. DERIVATION OF QUANTUM STATISTICAL HIERARCHY EQUATION

To explain how the quantum statistical effects appear in this formalism, we take as an example the Fourier coefficient $\rho_{k_1,k_2}(\boldsymbol{p}_1,\boldsymbol{p}_2|\boldsymbol{p}_3,\ldots,\boldsymbol{p}_N;t)$ with $\boldsymbol{k}_1+\boldsymbol{k}_2 \neq 0$. From (9), we have

$$\begin{aligned}&\rho_{k_1,k_2}(\boldsymbol{p}_1,\boldsymbol{p}_2|\boldsymbol{p}_3,\ldots,\boldsymbol{p}_N;t) \\ &= \Omega^2\rho^{(N)}\left(\boldsymbol{p}_1+\frac{\hbar}{2}\boldsymbol{k}_1,\boldsymbol{p}_2+\frac{\hbar}{2}\boldsymbol{k}_2,\boldsymbol{p}_3,\ldots,\boldsymbol{p}_N;\right. \\ &\quad\left.\boldsymbol{p}_1-\frac{\hbar}{2}\boldsymbol{k}_1,\boldsymbol{p}_2-\frac{\hbar}{2}\boldsymbol{k}_2,\boldsymbol{p}_3,\ldots,\boldsymbol{p}_N;t\right)\exp\left[i(\boldsymbol{k}_1\boldsymbol{p}_1+\boldsymbol{k}_2\boldsymbol{p}_2)\frac{t}{m}\right] \qquad (12)\end{aligned}$$

In (12), if $\boldsymbol{p}_1 + (\hbar/2)\boldsymbol{k}_1 = \boldsymbol{p}_2 - (\hbar/2)\boldsymbol{k}_2$, we can rewrite the right-hand side as

$$\delta^{\kappa}\left(\boldsymbol{p}_2 - \boldsymbol{p}_1 - \frac{\hbar}{2}\boldsymbol{k}_1 - \frac{\hbar}{2}\boldsymbol{k}_2\right) \times \Omega^2 \rho^{(N)}\left(\boldsymbol{p}_1 + \frac{\hbar}{2}\boldsymbol{k}_1, \boldsymbol{p}_2 + \frac{\hbar}{2}\boldsymbol{k}_2, \ldots; \boldsymbol{p}_2 - \hbar\boldsymbol{k}_1 - \frac{\hbar}{2}\boldsymbol{k}_2, \boldsymbol{p}_1 + \frac{\hbar}{2}\boldsymbol{k}_1, \ldots; t\right) \times \exp\left[i(\boldsymbol{k}_1 + \boldsymbol{k}_2)\left(\boldsymbol{p}_2 - \frac{\hbar}{2}\boldsymbol{k}_1\right)\frac{t}{m}\right] \tag{13}$$

where the notation $\delta^{\kappa}(\boldsymbol{p})$ indicates the product of three Kronecker deltas $\delta^{\kappa}_{p_x 0}\delta^{\kappa}_{p_y 0}\delta^{\kappa}_{p_z 0}$. Interchanging the momentum argument $\boldsymbol{p}_2 - \hbar\boldsymbol{k}_1 - \frac{1}{2}\hbar\boldsymbol{k}_2$ with $\boldsymbol{p}_1 + \frac{1}{2}\hbar\boldsymbol{k}_1$ in $\rho^{(N)}$ of (13), we can rewrite it with (9) as

$$\theta\Omega\, \delta^{\kappa}\left(\boldsymbol{p}_2 - \boldsymbol{p}_1 - \frac{\hbar}{2}\boldsymbol{k}_1 - \frac{\hbar}{2}\boldsymbol{k}_2\right) \exp\left[-\frac{\hbar}{2}\boldsymbol{k}_1 \boldsymbol{D}_{21}\right] \rho_{\boldsymbol{k}_1+\boldsymbol{k}_2}(\boldsymbol{p}_2 | \boldsymbol{p}_1, \boldsymbol{p}_3, \ldots; t) \tag{14}$$

where the statistical factor θ is equal to $+1$ for bosons and -1 for fermions. This example shows that, for certain values of momenta, the spatial correlation in $\rho_{\boldsymbol{k}_1,\boldsymbol{k}_2}$ is reduced to the lower one in $\rho_{\boldsymbol{k}_1+\boldsymbol{k}_2}$. This reduction is the quantum statistical effect called "contraction."[2] Similar contractions occur in (12) for the cases of $\boldsymbol{p}_1 - (\hbar/2)\boldsymbol{k}_1 = \boldsymbol{p}_2 + (\hbar/2)\boldsymbol{k}_2$ with $\boldsymbol{k}_1 + \boldsymbol{k}_2 \neq 0$ and of $\boldsymbol{p}_1 = \boldsymbol{p}_2$ with $\boldsymbol{k}_1 + \boldsymbol{k}_2 = 0$.

The general contractions in $\rho_{\boldsymbol{k}_1,\ldots,\boldsymbol{k}_r}$ are achieved in the following ways: First, the contraction between any two particles having nonzero wave vectors in $\rho_{\boldsymbol{k}_1,\ldots,\boldsymbol{k}_r}$ by the following formulas.

(i) For $\boldsymbol{k}_j + \boldsymbol{k}_n \neq 0$,

$$\begin{aligned}\rho_{\boldsymbol{k}_j,\boldsymbol{k}_n,\{k\}}(\boldsymbol{p}_j, \boldsymbol{p}_n, \{\boldsymbol{p}\}|\ldots) = {} & \rho'_{\boldsymbol{k}_j,\boldsymbol{k}_n,\{k\}}(\boldsymbol{p}_j, \boldsymbol{p}_n, \{\boldsymbol{p}\}|\ldots) \\ & + \theta\Omega\, \delta^{\kappa}\left(\boldsymbol{p}_j - \boldsymbol{p}_n - \frac{\hbar}{2}\boldsymbol{k}_j - \frac{\hbar}{2}\boldsymbol{k}_n\right) \\ & \times \exp\left[-\frac{\hbar}{2}\boldsymbol{k}_n \boldsymbol{D}_{jn}\right] \rho_{\boldsymbol{k}_j+\boldsymbol{k}_n,\{k\}}(\boldsymbol{p}_j, \{\boldsymbol{p}\}|\boldsymbol{p}_n, \ldots) \\ & + \theta\Omega\, \delta^{\kappa}\left(\boldsymbol{p}_n - \boldsymbol{p}_j - \frac{\hbar}{2}\boldsymbol{k}_j - \frac{\hbar}{2}\boldsymbol{k}_n\right) \\ & \times \exp\left[-\frac{\hbar}{2}\boldsymbol{k}_j \boldsymbol{D}_{nj}\right] \rho_{\boldsymbol{k}_j+\boldsymbol{k}_n,\{k\}}(\boldsymbol{p}_n, \{\boldsymbol{p}\}|\boldsymbol{p}_j, \ldots)\end{aligned} \tag{15a}$$

(ii) For $\boldsymbol{k}_j + \boldsymbol{k}_n = 0$,

$$\begin{aligned}\rho_{\boldsymbol{k}_j,\boldsymbol{k}_n,\{k\}}(\boldsymbol{p}_j, \boldsymbol{p}_n, \{\boldsymbol{p}\}|\ldots) & = \rho'_{\boldsymbol{k}_j,\boldsymbol{k}_n,\{k\}}(\boldsymbol{p}_j, \boldsymbol{p}_n, \{\boldsymbol{p}\}|\ldots) \\ & + \theta\Omega\, \delta^{\kappa}(\boldsymbol{p}_j - \boldsymbol{p}_n) \exp\left[-\frac{\hbar}{2}\boldsymbol{k}_n \boldsymbol{D}_{jn}\right] \rho_{\{k\}}(\{\boldsymbol{p}\}|\boldsymbol{p}_j, \boldsymbol{p}_n, \ldots)\end{aligned} \tag{15b}$$

where the prime on ρ indicates that the contractible parts between the wave vectors $\boldsymbol{k}_j$ and $\boldsymbol{k}_n$ in ρ are removed. We continue this procedure for the remaining wave vectors until all contractible parts are separated. Finally, we can express ρ in terms of a new Fourier coefficient $\tilde{\rho}$, which is defined as having no contractible parts in ρ. The coefficients ρ_0 and ρ_{k_j} contain no contractible parts, so

$$\begin{aligned}\tilde{\rho}_0(|\boldsymbol{p}_1,\ldots,\boldsymbol{p}_N) &= \rho_0(|\boldsymbol{p}_1,\ldots,\boldsymbol{p}_N)\\ \tilde{\rho}_{k_j}(\boldsymbol{p}_j|\boldsymbol{p}_1,\ldots,\boldsymbol{p}_{j-1},\boldsymbol{p}_{j+1},\ldots,\boldsymbol{p}_N) &= \rho_{k_j}(\boldsymbol{p}_j|\boldsymbol{p}_1,\ldots,\boldsymbol{p}_{j-1},\boldsymbol{p}_{j+1},\ldots,\boldsymbol{p}_N)\end{aligned} \tag{16}$$

To see the role of the contraction in the perturbation theory, we consider, as an example, the second-order contribution to $\rho_0(|\boldsymbol{p}_1,\boldsymbol{p}_2,\ldots;t)$ from $\rho_{l+l',-l-l'}(\boldsymbol{p}_1,\boldsymbol{p}_2|\ldots;0)$ in the iterated expansion of (10), that is,

$$\begin{aligned}&(i/\hbar)^2\Omega^{-2}\sum_l\sum_{l'}\int_0^t dt_1\int_0^{t_1}dt_2\{v(l)\exp[\tfrac{1}{2}\hbar\boldsymbol{l}\boldsymbol{D}_{12}^{(+)}]\\ &\quad - v(l)\exp[-\tfrac{1}{2}\hbar\boldsymbol{l}\boldsymbol{D}_{12}^{(-)}]\}\\ &\quad\times\exp[-i\boldsymbol{l}(\boldsymbol{p}_1-\boldsymbol{p}_2)(t_1-t_2)/m]\{v(l')\\ &\quad\times\exp[-\tfrac{1}{2}\hbar\boldsymbol{l}'\boldsymbol{D}_{12}^{(+)}] - v(l')\exp[-\tfrac{1}{2}\hbar\boldsymbol{l}'\boldsymbol{D}_{12}^{(-)}]\}\\ &\quad\times\exp[-i(\boldsymbol{l}+\boldsymbol{l}')(\boldsymbol{p}_1-\boldsymbol{p}_2)t_2/m]\rho_{l+l',-l-l'}(\boldsymbol{p}_1,\boldsymbol{p}_2|\ldots;0)\end{aligned} \tag{17}$$

This term appears to be a nondiagonal transition, but it contains implicitly the diagonal transition due to the quantum statistical effect and its contribution grows with time. That is, the Kronecker delta of the contracted part $\theta\Omega\,\delta^{\kappa}(\boldsymbol{p}_1-\boldsymbol{p}_2)\rho_0(|\boldsymbol{p}_1,\boldsymbol{p}_2,\ldots;0)$ in $\rho_{l+l',-l-l'}$ restricts the momentum arguments to be zero in the exponent of the rightmost propagator $\exp[-i(\boldsymbol{l}+\boldsymbol{l}')(\boldsymbol{p}_1-\boldsymbol{p}_2)t_2/m]$ in (17), and hence by the well-known asymptotic formula,

$$\exp\left[i\boldsymbol{l}\frac{\boldsymbol{p}}{m}t\right]\int_0^t dt_1 t_1{}^n\exp\left[-i\boldsymbol{l}\frac{\boldsymbol{p}}{m}t_1\right] = \frac{t^n}{i[\boldsymbol{l}(\boldsymbol{p}/m)-i\eta]},\qquad \eta\to 0+ \tag{18}$$

this contracted part gives the contribution proportional to the macroscopic time t.

Due to the existence of these implicit diagonal transitions as in this example, it is much more convenient to construct the hierarchy equation for $\tilde{\rho}_{\{k\}}(p;t)$ rather than $\rho_{\{k\}}(p;t)$. In $\tilde{\rho}_{\{k\}}(p;t)$ all parts bringing these diagonal transitions are separated out and this makes it possible to treat directly these diagonal transitions in the perturbation theory. This equation is just the quantum statistical hierarchy equation, and, as will be discussed soon, it will be given in the following form:

$$\begin{aligned}(\partial/\partial t)\,\tilde{\rho}_{\{k\}}(p;t) = &\sum_{j<n}^{N}\sum_{\{k'\}}\exp[i\sum_i \boldsymbol{k}_i\boldsymbol{p}_i t/m]\langle\{\boldsymbol{k}\}|\mathscr{M}_{jn}|\{\boldsymbol{k}'\}\rangle\\ &\times\exp[-i\sum_l \boldsymbol{k}_l'\boldsymbol{p}_l t/m]\Omega^{\nu-\nu'}\tilde{\rho}_{\{k'\}}(p;t)\end{aligned} \tag{19}$$

where the vertices $\langle\{\boldsymbol{k}\}|\mathscr{M}_{jn}|\{\boldsymbol{k}'\}\rangle$ are effective interactions, which come from the original interactions in (10) and the quantum statistical effects.

Now we discuss the derivation of this equation by a method based on the use of a diagrammatic method to treat the iterated expansion of (10) with the contraction. By the systematic use of the diagrammatic method, we can avoid any confusion due to the great number of combinations of the particles to be contracted, and, further, based on the concept of the moving contraction, we can avoid the double counting of the diagonal transitions due to the quantum statistical effects. We explain the method here, and give the details in the appendix.

First, we perform the contractions at the initial states, $\rho_{\{k\}}(p;0)$, in the iterated solution of (10) and we let the displacement operators in the vertex parts of (10) act on the Kronecker deltas appearing in the contractions. [See (A.3) in the appendix.] Then, we find that some of the contractions may be regarded as being performed at the intermediate states over these vertices. [See (A.5) and (A.6) in the appendix.] We refer to this fact by saying that "the contractions move over the vertices." Further, we let all contractions move over the vertices as successively as possible as they move toward the final state. In this process, we find that the unmovable contractions are of finite number and so the procedure of successive contractions can be closed, as will be seen in the appendix. Recalling here that $\tilde{\rho}_{\{k\}}(p;t)$ contains no contractible parts, we remove the terms in which any one of the contractions could move over all vertices. Then, the sum of the remaining terms is just $\tilde{\rho}_{\{k\}}(p;t)$ which has to be coincident with the iterated expansion of (19). By comparing them we can finally obtain the expressions of the vertices $\langle\{\boldsymbol{k}\}|\mathscr{M}_{jn}|\{\boldsymbol{k}'\}\rangle$, which consist of the original vertices in (10) and the Kronecker deltas of the contraction being unmovable over these original vertices.

We list the new vertices obtained by the above procedure in Table I. In this table the new vertices are classified according to the number of nonzero wave vectors on both sides of them. We find 11 elementary types of vertices. The vertices $\hat{\boldsymbol{a}}$ through $\hat{\boldsymbol{f}}$ correspond to those in classical systems,[1] but contain the quantum statistical effects. The vertex $\hat{\boldsymbol{g}}$ describes the forward collision. The vertices $\hat{\boldsymbol{h}}$ through $\hat{\boldsymbol{l}}$ are peculiar to the quantum statistics and they show the characteristic property that three or four particles can be affected through a single effective vertex.[4]

We refer here to the density dependence of each vertex in Table I. In physical problems, we are interested in the reduced distribution functions (7), which depend on the finite number of variables. Thus we have to regard that all momentum arguments except those of the fixed particles in the

[4] We remark that the results of the effective vertices given by Balescu in Ref. 2 contain errors, and further the vertices $\hat{\boldsymbol{k}}$ and $\hat{\boldsymbol{l}}$ in Table I have been overlooked.

vertices should be summed in actual treatments. After such a reduction, we see that each vertex brings two kinds of density dependence, which come from different origins. The first is due to the fact that the destruction of the spatial correlation of a particle through the collision with any one of N particles occurs accompanied by a special wave vector transfer, so that the probability of the process is proportional to N and Ω^{-1}. We list this kind of density dependence of each vertex in Table I. The second is due to the quantum statistical effects, namely the fact that the contracted terms always contain the Kronecker delta of momenta together with the summation over particles. For example, $\sum_r^N \delta^\kappa(\boldsymbol{p}_r - \boldsymbol{p}_1 + (\hbar/2)\boldsymbol{k}_1)$ in the vertex $\hat{\boldsymbol{a}}$ leads to a factor $h^3 c$ after the summation over the momentum as

$$\sum_r^N h^3 \Omega^{-1} \sum_{\boldsymbol{p}_r} \delta^\kappa\left(\boldsymbol{p}_1 - \boldsymbol{p}_r - \frac{\hbar}{2}\boldsymbol{k}_1\right) \approx h^3 c \tag{20}$$

This density dependence is related to the dimensionless parameter $\lambda_B{}^3 c$, where λ_B is the mean de Broglie wavelength.

3. MASTER EQUATION

As an application of Eq. (19), we will discuss briefly a general method to derive a generalized master equation of the momentum distribution function $\phi_N(\boldsymbol{p}_1,\ldots,\boldsymbol{p}_N; t)$ describing the system in which multiple collisions cannot be neglected and the mean de Broglie wavelength is not small as compared with the range of interaction.

Equation (19) has the same structure as the classical one, so we can proceed to obtain the master equation by the use of the diagrammatic method of Prigogine and Balescu.[1] In this method, each propagator of the particles having nonzero wave vector is indicated by a solid line running to left from right (this means that time is going to left from right), which is labeled with the index of the particle. Concerning particles having zero wave vectors, we draw nothing. Each of the 11 types of interaction $\langle\{\boldsymbol{k}\}|\mathscr{M}_{jn}|\{\boldsymbol{k}'\}\rangle$ in (19) is represented by a "vertex" connecting lines, which is shown in Table I.

In the iterated solution of (19), the topological structures of the diagrams correspond well with their time dependence, as is well known.[7] From (7), (8), and (16), we see that

$$\phi_N(\boldsymbol{p}_1,\ldots,\boldsymbol{p}_N; t) = \tilde{\rho}_0(|\boldsymbol{p}_1,\ldots,\boldsymbol{p}_N; t) \tag{21}$$

so we mention here only the time dependences of the diagrams relating to $\tilde{\rho}_0(p; t)$. The content of a diagram is separated into two regions as follows: The first is the "diagonal region," where, if it consists of l "diagonal fragments," it gives rise to the time dependence $t^l/l!$. The second is the "destruc-

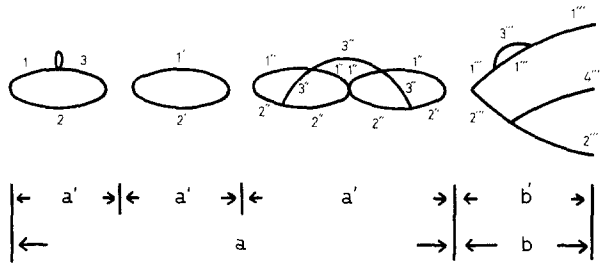

Fig. 1. (a) Diagonal region; (a′) diagonal fragment. (b) Destruction region; (b′) destruction fragment.

tion region," consisting of only one "destruction fragment," which does not give rise to the growing contribution with time. An example of a diagram consisting of three diagonal fragments accompanied by a destruction fragment is shown in Fig. 1.

Now we discuss the parameters characterizing the system to classify the diagrams in the iterated expansion of (19). In our system, the density c is a good parameter and, as we have seen, there are two kinds of density dependences which come from the vertices in Table I. The first is due to the collision and it brings about the factor c^{m-1} if m particles are encountered in their interaction ranges at the same time. The second is the h^3c dependence due to the quantum statistical effects through the contraction, and we will take full account of these quantum effects. Further, in treating the long-time behavior of the system as compared with the duration of a collision, time t becomes another parameter to classify the expanded terms of (19). As has been discussed above, a time factor t is brought in through a diagonal fragment. So if the diagonal fragment contains m particles, it gives rise to a contribution of the order $(c^{m-1}t)(h^3c)^s$, where $s = 0, 1, 2....$ Furthermore, corresponding to the existence of r-body correlation at the initial time, i.e., $\tilde{\rho}_{k_1,\ldots,k_r}(p; 0) \neq 0$, the extra factor $c^u(h^3c)^s$ is brought in through the destruction fragment, where $u \geq r - 1$. Consequently, to get our master equation involving up to n-body collisions, we sum the diagrams of the order

$$(ct)^{q_1}(c^2t)^{q_2} \cdots (c^{n-1}t)^{q_{n-1}}c^u(h^3c)^s \tag{22}$$

in the iterated expansion of (19). Here q_j is the number of diagonal fragments containing $j + 1$ particles in the diagram, where $q_1,\ldots, q_{n-1} = 0, 1, 2,....$ An example of these diagrams is shown in Fig. 1, which has the order of $(ct)(c^2t)^2c^3$ except for the h^3c dependence.

We can now derive our quantum statistical master equation from (19) in accordance with the general procedure developed by Prigogine and his

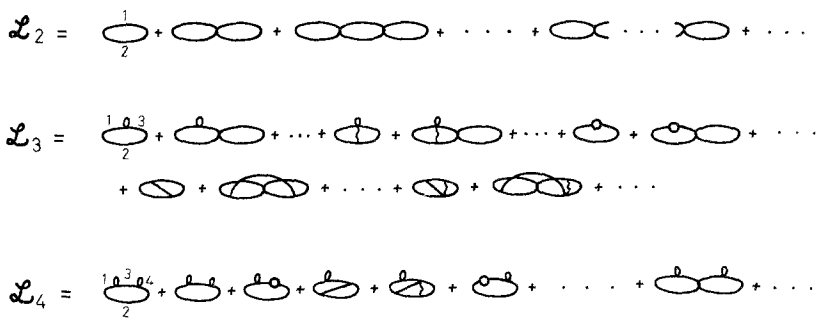

Fig. 2. Sum of diagonal fragments.

collaborators[1,2,7] for classical systems. The derivation is as follows. First, we write down all diagrams of the order (22) relating to $\tilde{\rho}_0(p;t)$ in the iterated solution of (19) and classify them into two groups according to whether or not they contain the diagonal fragment. In the former group, we factor out the sum of all of the diagonal fragments located at the leftmost side of each diagram, and then we find that the remaining part is just $\tilde{\rho}_0$. After the time derivative is taken the diagrams belonging to the latter group vanish because they have no time dependence. Thus, we can obtain the quantum statistical master equation in the form

$$(\partial/\partial t)\phi_N(p;t) = \sum_{m=2}^{n} \mathscr{L}_m \phi_N(p;t) \tag{23}$$

where $\mathscr{L}_m$ is the sum of the terms corresponding to all diagonal fragments (except the time factor) of the order $c^{m-1}(h^3c)^s$.

The first few diagonal fragments appearing in the kernel of the master equation $\mathscr{L}_m$ are shown in Fig. 2.

In order to see how the quantum statistical effects appear in our formalism, we give here the expression of the master equation (23) for the simple case of $m = 2, 3$. The kernel of our master equation can contain an arbitrary number of vertices $\hat{e}$, as shown in Fig. 2, because it is irrelevant to the parameters characterizing our system. Then, by introducing the propagator G_2 represented in diagram form in Fig. 3b, we get the following result for $\mathscr{L}_2$:

$$\mathscr{L}_2 = \sum_{1<2}^{N} \langle 0|\hat{\boldsymbol{e}}_{12} G_2 \hat{\boldsymbol{a}}_{12}|0\rangle \tag{24}$$

where the two-body propagator G_2 satisfies the integral equation

$$G_2 = G_0^{(2)} + G_0^{(2)} \hat{\boldsymbol{e}}_{12} G_2 \tag{25}$$

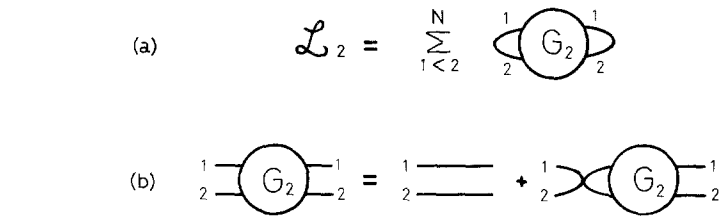

Fig. 3. (a) Compact expression of the kernel $\mathscr{L}_2$. (b) Two-body propagator G_2.

The two-body free propagator $G_0^{(2)}$ is defined by

$$\langle \boldsymbol{k}_1, \boldsymbol{k}_2 | G_0^{(2)} | \boldsymbol{k}'_1, \boldsymbol{k}_2' \rangle = \frac{1}{i\{(\boldsymbol{k}_1 p_1 + \boldsymbol{k}_2 p_2)/m - i\eta\}} \delta^\kappa(\boldsymbol{k}_1 - \boldsymbol{k}_1')\delta^\kappa(\boldsymbol{k}_2 - \boldsymbol{k}_2') \tag{26}$$

which appears after integrating over times in the iterated expansion of (19) by the use of the asymptotic formula (18). The corresponding diagrams to (24) and (25) are shown in Fig. 3. Similarly, we can obtain for $\mathscr{L}_3$

$$\begin{aligned}
\mathscr{L}_3 = \sum_{1,2,3}^{N} \{ & \langle 0|\hat{\boldsymbol{c}}_{12} G_2 \hat{\boldsymbol{f}}_{13} G_2 \hat{\boldsymbol{a}}_{23}|0\rangle + \langle 0|\hat{\boldsymbol{c}}_{12} G_2 \hat{\boldsymbol{h}}_{13} G_2 \hat{\boldsymbol{a}}_{23}|0\rangle \\
& + \langle 0|\hat{\boldsymbol{c}}_{12} G_2 \hat{\boldsymbol{g}}_{13} G_2 \hat{\boldsymbol{a}}_{12}|0\rangle \\
& + [\langle 0|\hat{\boldsymbol{c}}_{12} G_2 \hat{\boldsymbol{d}}_{13} G_3 \hat{\boldsymbol{b}}_{13} G_2 \hat{\boldsymbol{a}}_{12}|0\rangle + \langle 0|\hat{\boldsymbol{c}}_{12} G_2 \hat{\boldsymbol{d}}_{13} G_3 \hat{\boldsymbol{b}}_{13} G_2 \hat{\boldsymbol{a}}_{23}|0\rangle \\
& + \langle 0|\hat{\boldsymbol{c}}_{12} G_2 \hat{\boldsymbol{d}}_{13} G_3 \hat{\boldsymbol{b}}_{12} G_2 \hat{\boldsymbol{a}}_{12}|0\rangle + \langle 0|\hat{\boldsymbol{c}}_{12} G_2 \hat{\boldsymbol{d}}_{13} G_3 \hat{\boldsymbol{b}}_{12} G_2 \hat{\boldsymbol{a}}_{23}|0\rangle \\
& + \langle 0|\hat{\boldsymbol{c}}_{12} G_2 \hat{\boldsymbol{d}}_{13} G_3 \hat{\boldsymbol{b}}_{23} G_2 \hat{\boldsymbol{a}}_{12}|0\rangle + \langle 0|\hat{\boldsymbol{c}}_{12} G_2 \hat{\boldsymbol{d}}_{13} G_3 \hat{\boldsymbol{b}}_{23} G_2 \hat{\boldsymbol{a}}_{13}|0\rangle \\
& + \langle 0|\hat{\boldsymbol{c}}_{12} G_2 \hat{\boldsymbol{d}}_{13} G_3 \hat{\boldsymbol{j}}_{13} G_2 \hat{\boldsymbol{a}}_{12}|0\rangle \\
& + (\text{five other terms in which the subscripts to the vertices are changed as in the preceding terms})]\}
\end{aligned} \tag{27}$$

where the three-body propagator G_3 satisfies the integral equation

$$G_3 = G_0^{(3)} + G_0^{(3)}(\hat{\boldsymbol{e}}_{12} + \hat{\boldsymbol{e}}_{23} + \hat{\boldsymbol{e}}_{13}) G_3 \tag{28}$$

and the three-body free propagator $G_0^{(3)}$ is defined by

$$\begin{aligned}
& \langle \boldsymbol{k}_1, \boldsymbol{k}_2, \boldsymbol{k}_3 | G_0^{(3)} | \boldsymbol{k}_1', \boldsymbol{k}_2', \boldsymbol{k}_3' \rangle \\
& = \frac{1}{i\{(\boldsymbol{k}_1 p_1 + \boldsymbol{k}_2 p_2 + \boldsymbol{k}_3 p_3)/m - i\eta\}} \delta^\kappa(\boldsymbol{k}_1 - \boldsymbol{k}_1')\delta^\kappa(\boldsymbol{k}_2 - \boldsymbol{k}_2')\delta^\kappa(\boldsymbol{k}_3 - \boldsymbol{k}_3')
\end{aligned} \tag{29}$$

The diagrams corresponding to (27) and (28) are shown in Fig. 4. The kernel $\mathscr{L}_3$ contains the vertices $\hat{\boldsymbol{g}}$, $\hat{\boldsymbol{h}}$, and $\hat{\boldsymbol{j}}$ peculiar to the quantum statistics.

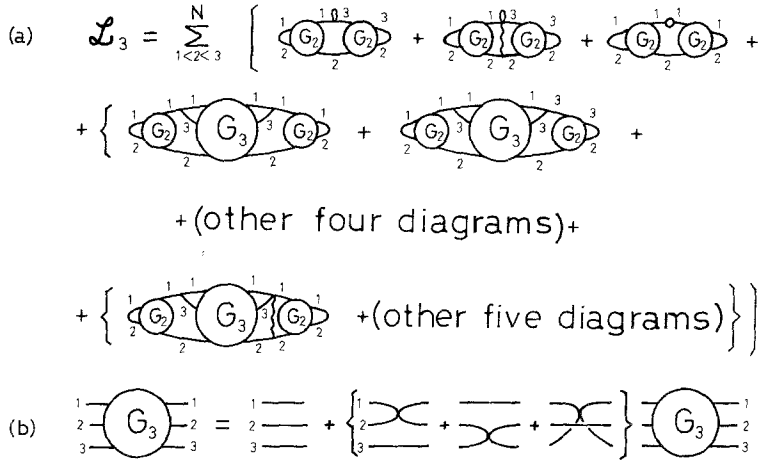

Fig. 4. (a) Compact expression of the kernel $\mathscr{L}_3$. (b) Three-body propagator G_3.

4. SUMMARY AND DISCUSSION

We started from the hierarchy equation (10), which is satisfied by the Fourier coefficient $\rho_{\{k\}}(p; t)$ for the Wigner distribution function. The new Fourier coefficient $\tilde{\rho}_{\{k\}}(p; t)$ was obtained from $\rho_{\{k\}}(p; t)$ by applying the contraction technique which was first used by Balescu and improved in this paper. The new hierarchy equation for $\tilde{\rho}_{\{k\}}(p; t)$ is derived in (19), in which the quantum statistical effects originating from the diagonal transition are incorporated into the effective vertices $\langle\{\boldsymbol{k}\}|\mathscr{M}_{jn}|\{\boldsymbol{k}'\}\rangle$.

Our method of obtaining $\tilde{\rho}_{\{k\}}(p; t)$ and the equation for $\tilde{\rho}_{\{k\}}(p; t)$ is characterized by the use of diagrams for the contraction procedure and also by the adoption of the concept of the moving contraction. By our method, complications in the contraction procedure are much reduced and any confusion of double counting for the diagonal transitions can be excluded systematically.

In our formalism, the main parts of the quantum statistical effects, which contribute to the long-time behavior of the system, are included in the effective vertices $\langle\{\boldsymbol{k}\}|\mathscr{M}_{jn}|\{\boldsymbol{k}'\}\rangle$. This is a general and favorable feature in that we can treat such quantum statistical effects directly by the perturbation theory and can take account of them into the calculations up to any desirable order.

Finally, we mention the recent work of the Brussels school. In particular, a general theory of subdynamics has been given by Prigogine *et al.*[8] and its extension has been given by Balescu for the quantum statistical systems in the cluster expansion formalism.[9] In this work, the quantum statistical effects are taken into account by constructing the effective Liouville operator

with the symmetrization operator on the frame of the cluster expansion. It is of interest to investigate the treatment of the quantum statistical effects in the formalism based on the cluster expansion in relation to that in our formalism based on the Fourier expansion method. This problem will be discussed elsewhere.

APPENDIX

In this appendix we give details of the diagrammatic method used to derive Eq. (19) with the effective vertices $\langle\{\boldsymbol{k}\}|\mathscr{M}_{jn}|\{\boldsymbol{k}'\}\rangle$ from Eq. (10), and we show how the calculation can be done systematically without double counting for the diagonal transition due to the quantum statistical effects. (We put $\hbar = 1$ and $m = 1$ for simplicity.)

A.1. Introduction of Diagram

First we start with the diagrammatic representation for terms of the iterated expansion of (10). We take as an example the first-order terms for $\exp[-i\boldsymbol{k}_1\boldsymbol{p}_1 t]\rho_{k_1}(\boldsymbol{p}_1|\boldsymbol{p}_2,\ldots;t)$ connecting to $\rho_{k_1+l,-l}(\boldsymbol{p}_1,\boldsymbol{p}_2|\ldots;0)$, i.e.,

$$
\begin{aligned}
& i\Omega^{-1}\sum_{l}\int_0^t dt_1 \exp[-i\boldsymbol{k}_1\boldsymbol{p}_1(t-t_1)] \\
& \quad\times\{v(l)\exp[-\tfrac{1}{2}l\boldsymbol{D}_{12}^{(+)}] - v(l)\exp[-\tfrac{1}{2}l\boldsymbol{D}_{12}^{(-)}]\} \\
& \quad\times\exp\{-i[(\boldsymbol{k}_1+\boldsymbol{l})\boldsymbol{p}_1 - \boldsymbol{l}\boldsymbol{p}_2]t\}\Omega^{-1}\boldsymbol{p}_{k_1+l,-l}(\boldsymbol{p}_1,\boldsymbol{p}_2|\cdots;0) \qquad \text{(A.1)}
\end{aligned}
$$

This is represented in Fig. 5. That is, we draw a horizontal solid line for each propagator $\exp[-i\boldsymbol{k}_j\boldsymbol{p}_j(t'-t'')]$ and put the argument $\boldsymbol{p}_j - \frac{1}{2}\boldsymbol{k}_j$ on this solid line. For the particles having zero wave vectors we draw nothing in general, but if necessary, we draw broken horizontal lines for them relating to the interaction or the contraction. The interactions $v(l)\exp[-\frac{1}{2}l\boldsymbol{D}_{12}^{(\pm)}]$ are represented by vertical wavy lines with an arrow connecting two horizontal lines and labeled with the notation $(+)$ $[(-)]$ corresponding to the operator $\boldsymbol{D}^{(+)}$ [the operator $\boldsymbol{D}^{(-)}$]. The orientation of the arrow is determined by the

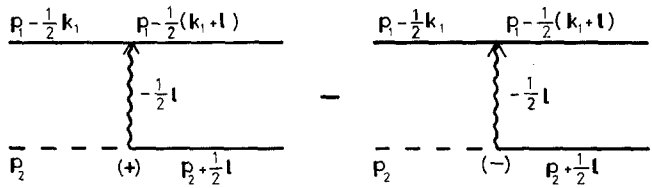

Fig. 5. Diagrams corresponding to (A.1).

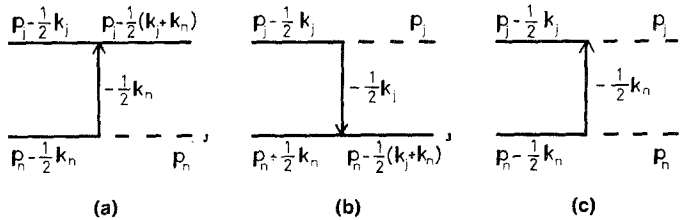

Fig. 6. Diagrams for contractions between particles j and n.

order of the subscripts jn of the operators $\boldsymbol{D}_{jn}^{(\pm)}$ as toward the particle j from the particle n. On the wavy line we put the wave vector $-\boldsymbol{l}/2$ such that the total wave vector is conserved from the left-hand side of the wavy line to the right-hand side.

A.2. Diagram for Contraction

Next, by formulas (15a) and (15b), the contractions for $\rho_{k_j,k_n,\{k\}}(\boldsymbol{p}_j, \boldsymbol{p}_n, \{\boldsymbol{p}\}| \cdots)$ are represented by the following rules: We draw vertical solid lines with an arrow connecting two horizontal lines for the contractions between the particles j and n. (See Fig. 6.) The orientation of the arrow is determined by the order of the subscripts jn of $\boldsymbol{D}_{jn}$ in (15a) and (15b) as toward j from n. We put the wave vector on the vertical solid line so that the total wave vector is conserved from the left-hand side of the vertical line to the right-hand side. The diagrams corresponding to the second and third terms in (15a) and the second term in (15b) are shown in (a), (b), and (c) of Fig. 6, respectively. There, the wave vector of the vertical solid line is just the one in the displacement operator, and the argument of the Kronecker delta in (15) is the difference between the arguments on the two horizontal lines of the right-hand side.

For the case of the contraction including more than two particles, the contraction can be performed by the successive use of formulas (15a) and (15b). In our diagrammatic representation, the vertical lines are arranged to right from left in accordance with the order of the contractions of two particles. (See Fig. 7.)

Here, we remark that the difference of the order in successive contrac-

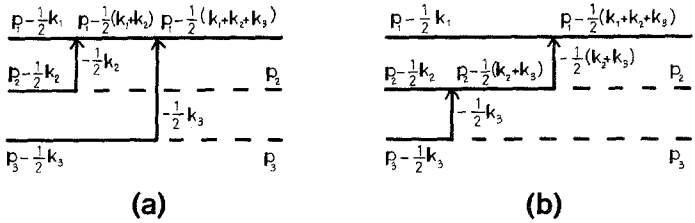

Fig. 7. Diagrams leading to equivalent contractions for $\rho_{k_1k_2k_3}$.

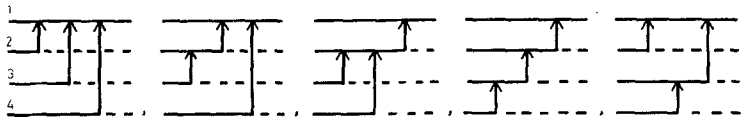

Fig. 8. Diagrams leading to equivalent contractions for $\rho_{k_1k_2k_3k_4}$.

tions does not always lead to a different result. That is, the two types of diagrams (a) and (b) in Fig. 7 give the same expression,

$$\theta^2\Omega^2\,\delta^{\kappa}(\boldsymbol{p}_1-\boldsymbol{p}_2-\tfrac{1}{2}\boldsymbol{k}_1-\tfrac{1}{2}\boldsymbol{k}_2)\,\delta^{\kappa}(\boldsymbol{p}_2-\boldsymbol{p}_3-\tfrac{1}{2}\boldsymbol{k}_2-\tfrac{1}{2}\boldsymbol{k}_3)\exp[-\tfrac{1}{2}\boldsymbol{k}_2\boldsymbol{D}_{12}]$$
$$\times\exp[-\tfrac{1}{2}\boldsymbol{k}_3\boldsymbol{D}_{13}]\rho_{k_1+k_2+k_3}(\boldsymbol{p}_1|\boldsymbol{p}_2,\boldsymbol{p}_3,\ldots) \tag{A.2}$$

and lead to equivalent contractions. Thus, it is necessary to take account of either one of them. For the general contraction including more than three particles, we can still use the above criterion for any two successive contractions. For example, as is easily seen, all diagram in Fig. 8 lead to the equivalent contraction for $\rho_{k_1k_2k_3k_4}(\boldsymbol{p}_1,\boldsymbol{p}_2,\boldsymbol{p}_3,\boldsymbol{p}_4|\cdots)$ to $\rho_{k_1+k_2+k_3+k_4}(\boldsymbol{p}_1|\boldsymbol{p}_2,\boldsymbol{p}_3,\boldsymbol{p}_4,\ldots)$ and only one of them has to be taken into account.

A.3. Derivation of Effective Vertices

We now illustrate how the effective vertices of (19) can be derived by the use of the diagrammatic method. As has been discussed in Section 2, the general procedure is as follows: To take out the part corresponding to $\tilde{\rho}_{\{k\}}(p;t)$ from the iterated expansion (10) for $\rho_{\{k\}}(p;t)$, the contractions are performed at the initial states $\rho_{\{k'\}}(p;0)$, and these contractions are moved, if possible, over the original vertices toward the final state. Then, if we get rid of the terms having the contraction at the final state, we can obtain just $\tilde{\rho}_{\{k\}}(p;t)$, which must be coincident with the iterated expansion of (19) with the effective vertices.

As an example, we first take the diagram shown in Fig. 9, which is the first-order term for $\rho_{k_1k_2}(\boldsymbol{p}_1,\boldsymbol{p}_2|\ldots;t)$ connecting to $\rho_{k_1+k_2}(\boldsymbol{p}_1|\boldsymbol{p}_2,\ldots;0)$ with

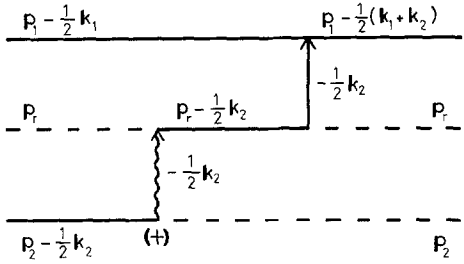

Fig. 9. One of the effective vertices.

a single contraction. From our rule, the explicit expression of this diagram can be written as

$$
\begin{aligned}
i\Omega^{-1}\sum_{r}^{N}\int_{0}^{t} dt_1 \exp[-i(\boldsymbol{k}_1\boldsymbol{p}_1 + \boldsymbol{k}_2\boldsymbol{p}_2)(t-t_1)]v(k_2) \\
\times \exp[-\tfrac{1}{2}\boldsymbol{k}_2\boldsymbol{D}_{r2}^{(+)}]\exp[-i(\boldsymbol{k}_1\boldsymbol{p}_1 + \boldsymbol{k}_2\boldsymbol{p}_r)t_1] \\
\times \theta\Omega\,\delta^{\kappa}(\boldsymbol{p}_1 - \boldsymbol{p}_r - \tfrac{1}{2}\boldsymbol{k}_1 - \tfrac{1}{2}\boldsymbol{k}_2)\exp[-\tfrac{1}{2}\boldsymbol{k}_2\boldsymbol{D}_{1r}]\tilde{\rho}_{k_1+k_2}(\boldsymbol{p}_1|\boldsymbol{p}_2,\boldsymbol{p}_r,\ldots;0)
\end{aligned}
\tag{A.3}
$$

The contraction in (A.3) does not become any one of the contraction performed in $\rho_{k_1k_2}(\boldsymbol{p}_1,\boldsymbol{p}_2|,\ldots;t)$ after operation of the displacement operator; therefore we cannot regard that this contraction moves over the vertex. This contraction is incorporated into the effective vertex. We rewrite (A.3) as

$$
\begin{aligned}
\int dt_1 \exp[-i(\boldsymbol{k}_1\boldsymbol{p}_1 + \boldsymbol{k}_2\boldsymbol{p}_2)(t-t_1)] \\
\times \{i\Omega^{-1}v(k_2)\theta\sum_{r}^{N}\delta^{\kappa}(\boldsymbol{p}_1 - \boldsymbol{p}_r - \tfrac{1}{2}\boldsymbol{k}_1)\exp[-\tfrac{1}{2}\boldsymbol{k}_2\boldsymbol{D}_{12}]\} \\
\times \exp[-i(\boldsymbol{k}_1 + \boldsymbol{k}_2)\boldsymbol{p}_1t_1]\Omega\tilde{\rho}_{k_1+k_2}(\boldsymbol{p}_1|\boldsymbol{p}_2,\boldsymbol{p}_r,\ldots;0)
\end{aligned}
\tag{A.4}
$$

then the expression in the curly bracket in (A.4) is just contribution to the effective vertex $\hat{\boldsymbol{b}}$ in Table I.

Next, we take as an example the second-order terms in Fig. 10 to illustrate the movable contraction over the vertex. This is expressed as

$$
\begin{aligned}
i^2\Omega^{-2}\sum_{r}^{N}\int_{0}^{t} dt_1\int_{0}^{t_1} dt_2 \exp[-i(\boldsymbol{k}_1\boldsymbol{p}_1 + \boldsymbol{k}_2\boldsymbol{p}_2 + \boldsymbol{k}_3\boldsymbol{p}_3)(t-t_1)] \\
\times v(k_2)\exp[-\tfrac{1}{2}\boldsymbol{k}_2\boldsymbol{D}_{r2}^{(+)}] \\
\times \exp[-i(\boldsymbol{k}_1\boldsymbol{p}_1 + \boldsymbol{k}_3\boldsymbol{p}_3 + \boldsymbol{k}_2\boldsymbol{p}_r)(t_1-t_2)]v(k_3) \\
\times \exp[-\tfrac{1}{2}\boldsymbol{k}_3\boldsymbol{D}_{r3}^{(+)}]\exp[i\{\boldsymbol{k}_1\boldsymbol{p}_1 + (\boldsymbol{k}_2+\boldsymbol{k}_3)\boldsymbol{p}_r\}t_2] \\
\times \theta\Omega\,\delta^{\kappa}(\boldsymbol{p}_1 - \boldsymbol{p}_r - \tfrac{1}{2}\boldsymbol{k}_1 - \tfrac{1}{2}\boldsymbol{k}_2 - \tfrac{1}{2}\boldsymbol{k}_3)\exp[-\tfrac{1}{2}(\boldsymbol{k}_2+\boldsymbol{k}_3)\boldsymbol{D}_{1r}] \\
\times \Omega\tilde{\rho}_{k_1+k_2+k_3}(\boldsymbol{p}_1|\boldsymbol{p}_2,\boldsymbol{p}_3,\boldsymbol{p}_r,\ldots;0)
\end{aligned}
\tag{A.5}
$$

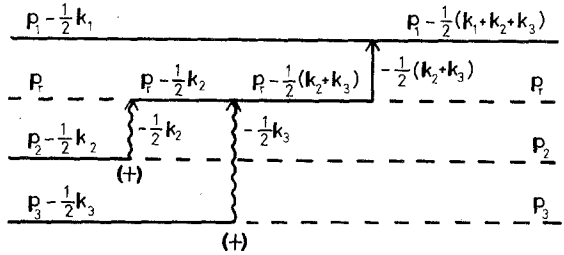

Fig. 10. Example of a movable contraction (before being moved).

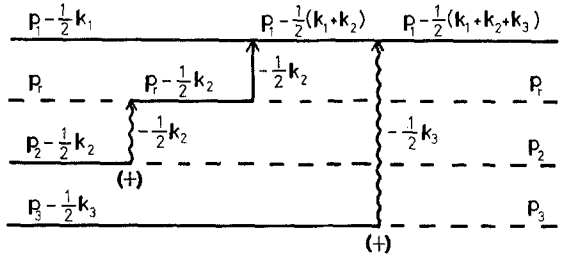

Fig. 11. Example of a movable contraction (after being moved).

If we rewrite (A.5) in the form

$$
\begin{aligned}
i^2\Omega^{-2}\sum_{r}^{N}\int_0^t dt_1\int_0^{t_1} dt_2\,&\exp[-i(\boldsymbol{k}_1\boldsymbol{p}_1+\boldsymbol{k}_2\boldsymbol{p}_2+\boldsymbol{k}_3\boldsymbol{p}_3)(t-t_1)]\\
&\times v(k_2)\exp[-\tfrac{1}{2}\boldsymbol{k}_2\boldsymbol{D}_{r2}^{(+)}]\\
&\times \exp[-i(\boldsymbol{k}_1\boldsymbol{p}_1+\boldsymbol{k}_3\boldsymbol{p}_3+\boldsymbol{k}_2\boldsymbol{p}_r)(t_1-t_2)]\\
&\times \theta\Omega\delta^{\kappa}(\boldsymbol{p}_1-\boldsymbol{p}_r-\tfrac{1}{2}\boldsymbol{k}_1-\tfrac{1}{2}\boldsymbol{k}_2)\exp[-\tfrac{1}{2}\boldsymbol{k}_2\boldsymbol{D}_{1r}]\\
&\times v(k_3)\exp[-\tfrac{1}{2}\boldsymbol{k}_3\boldsymbol{D}_{13}^{(+)}]\exp[-i(\boldsymbol{k}_1+\boldsymbol{k}_2+\boldsymbol{k}_3)\boldsymbol{p}_1t_2]\\
&\times \Omega\tilde{\rho}_{k_1+k_2+k_3}(\boldsymbol{p}_1|\boldsymbol{p}_2,\boldsymbol{p}_3,\boldsymbol{p}_r,\ldots;0)
\end{aligned}
\tag{A.6}
$$

this term can be represented by the diagram in Fig. 11. This shows that the contraction in (A.5) moves over the vertex and it becomes the contraction being performed at the intermediate state. By incorporating this contraction with the left-hand vertex, we again arrive at the same expression obtained in (A.4).

There are not so many types of movable contractions. In Fig. 12, we show all types of contractions that can move over the original vertex of (10). Here, the pairs of diagrams are the same.

Thus, on the basis of our diagrammatic method, we can now easily construct all effective vertices listed in Table I. We list in Table II the diagrams containing the vertex of (+) in (10), which correspond to the first terms in the expressions in Table I.

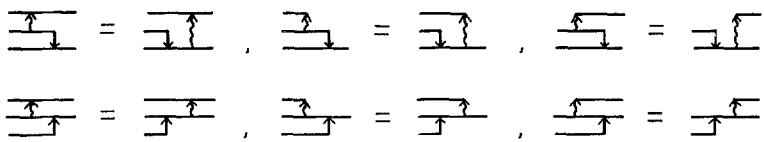

Fig. 12. All types of contractions that can move over the original vertex in (10). The interaction in figures on the upper and lower lines is the (+) vertex and the (−) vertex, respectively.

Table I. Effective Vertices[a]

Vertex	Prigogine–Balescu diagram	Density dependence due to collision	Effective interaction
$\hat{a}_{12}$		—	$\langle \boldsymbol{k}_1, \boldsymbol{k}_2 \vert \mathscr{M}_{12} \vert 0 \rangle = i\hbar^{-1}\Omega^{-1}\,\delta^{\kappa}(\boldsymbol{k}_1 + \boldsymbol{k}_2)[A(\boldsymbol{k}_1, \boldsymbol{k}_2) - A(-\boldsymbol{k}_1, -\boldsymbol{k}_2)]$ $A(\boldsymbol{k}_1, \boldsymbol{k}_2) = [v(k_1) + \theta v(\vert \boldsymbol{p}_1 - \boldsymbol{p}_2 \vert/\hbar)][1 + \theta \sum_r \delta^{\kappa}(\boldsymbol{p}_1 - \boldsymbol{p}_r - \tfrac{1}{2}\hbar\boldsymbol{k}_1)]$ $\times [1 + \theta \sum_s \delta^{\kappa}(\boldsymbol{p}_2 - \boldsymbol{p}_s - \tfrac{1}{2}\hbar\boldsymbol{k}_2)] \exp(\tfrac{1}{2}\hbar\boldsymbol{k}_1 \boldsymbol{D}_{12})$
$\hat{b}_{12}$	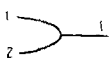	—	$\langle \boldsymbol{k}_1, \boldsymbol{k}_2 \vert \mathscr{M}_{12} \vert \boldsymbol{k}_1' \rangle = i\hbar^{-1}\Omega^{-1}\,\delta^{\kappa}(\boldsymbol{k}_1' - \boldsymbol{k}_1 - \boldsymbol{k}_2)[B(\boldsymbol{k}_1, \boldsymbol{k}_2) - B(-\boldsymbol{k}_1, -\boldsymbol{k}_2)]$ $B(\boldsymbol{k}_1, \boldsymbol{k}_2) = [v(k_2) + \theta v(\vert \boldsymbol{p}_1 - \boldsymbol{p}_2 - \tfrac{1}{2}\hbar\boldsymbol{k}_1 - \tfrac{1}{2}\hbar\boldsymbol{k}_2 \vert/\hbar)]$ $\times [1 + \theta \sum_r \delta^{\kappa}(\boldsymbol{p}_1 - \boldsymbol{p}_r - \tfrac{1}{2}\hbar\boldsymbol{k}_1)][1 + \theta \sum_s \delta^{\kappa}(\boldsymbol{p}_2 - \boldsymbol{p}_s - \tfrac{1}{2}\hbar\boldsymbol{k}_2)]$ $\times [\exp(-\tfrac{1}{2}\hbar\boldsymbol{k}_2 \boldsymbol{D}_{12})] + [v(k_2) + \theta v(\vert \boldsymbol{p}_1 - \boldsymbol{p}_2 + \tfrac{1}{2}\hbar\boldsymbol{k}_1 + \tfrac{1}{2}\hbar\boldsymbol{k}_2 \vert/\hbar)]$ $\times \theta \sum_r \delta^{\kappa}(\boldsymbol{p}_1 - \boldsymbol{p}_r + \tfrac{1}{2}\hbar\boldsymbol{k}_1 + \tfrac{1}{2}\hbar\boldsymbol{k}_2)[1 + \theta \sum_s \delta^{\kappa}(\boldsymbol{p}_2 - \boldsymbol{p}_s - \tfrac{1}{2}\hbar\boldsymbol{k}_2)]$ $\times \exp(\tfrac{1}{2}\hbar\boldsymbol{k}_2 \boldsymbol{D}_{1r}) \exp(\tfrac{1}{2}\hbar\boldsymbol{k}_2 \boldsymbol{D}_{2r})$
$\hat{c}_{jn}$	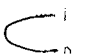	c	$\langle 0 \vert \mathscr{M}_{jn} \vert \boldsymbol{k}_j', \boldsymbol{k}_n' \rangle = i\hbar^{-1}\Omega^{-1} \sum_l \delta^{\kappa}(\boldsymbol{k}_j' - \boldsymbol{l})\,\delta^{\kappa}(\boldsymbol{k}_n' + \boldsymbol{l})$ $\times [v(l) \exp(-\tfrac{1}{2}\hbar l \boldsymbol{D}_{jn}) - v(l) \exp(\tfrac{1}{2}\hbar l \boldsymbol{D}_{jn})]$
$\hat{d}_{1n}$		c	$\langle \boldsymbol{k}_1 \vert \mathscr{M}_{1n} \vert \boldsymbol{k}_1', \boldsymbol{k}_n' \rangle = i\hbar^{-1}\Omega^{-1} \sum_l \delta^{\kappa}(\boldsymbol{k}_1' - \boldsymbol{k}_1 - \boldsymbol{l})$ $\times \delta^{\kappa}(\boldsymbol{k}_n' + \boldsymbol{l})[\mathrm{D}(\boldsymbol{k}_1, \boldsymbol{l}) - \mathrm{D}(-\boldsymbol{k}_1, -\boldsymbol{l})]$ $\mathrm{D}(\boldsymbol{k}_1, \boldsymbol{l}) = v(l)[1 + \theta \sum_r \delta^{\kappa}(\boldsymbol{p}_1 - \boldsymbol{p}_r - \tfrac{1}{2}\hbar\boldsymbol{k}_1)] \exp(-\tfrac{1}{2}\hbar l \boldsymbol{D}_{1n}) + v(l)$ $\times \theta \sum_r \delta^{\kappa}(\boldsymbol{p}_1 - \boldsymbol{p}_r + \tfrac{1}{2}\hbar\boldsymbol{k}_1 + \hbar\boldsymbol{l}) \exp(\tfrac{1}{2}\hbar l \boldsymbol{D}_{1r}) \exp(\tfrac{1}{2}\hbar l \boldsymbol{D}_{nr})$

Table I. Continued

Vertex	Prigogine–Balescu diagram	Density dependence due to collision	Effective interaction
$\hat{e}_{12}$		—	$\langle \boldsymbol{k}_1,\boldsymbol{k}_2\|\mathscr{M}_{12}\|\boldsymbol{k}_1',\boldsymbol{k}_2'\rangle = i\hbar^{-1}\Omega^{-1}\sum_{\boldsymbol{l}}\delta^{\kappa}(\boldsymbol{k}_1'-\boldsymbol{k}_1-\boldsymbol{l})\,\delta^{\kappa}(\boldsymbol{k}_2'-\boldsymbol{k}_2+\boldsymbol{l})$ $\times[\mathrm{E}(\boldsymbol{k}_1,\boldsymbol{k}_2,\boldsymbol{l})-\mathrm{E}(-\boldsymbol{k}_1,-\boldsymbol{k}_2,-\boldsymbol{l})]$ $\mathrm{E}(\boldsymbol{k}_1,\boldsymbol{k}_2,\boldsymbol{l}) = v(l)[1+\theta\sum_{r}\delta^{\kappa}(\boldsymbol{p}_1-\boldsymbol{p}_r-\tfrac{1}{2}\hbar\boldsymbol{k}_1)][1+\theta\sum_{s}\delta^{\kappa}(\boldsymbol{p}_2-\boldsymbol{p}_s-\tfrac{1}{2}\hbar\boldsymbol{k}_2)]$ $\times\exp(-\tfrac{1}{2}\hbar\boldsymbol{l}\boldsymbol{D}_{12})+v(l)\theta\sum_{r}\delta^{\kappa}(\boldsymbol{p}_1-\boldsymbol{p}_r+\tfrac{1}{2}\hbar\boldsymbol{k}_1+\hbar\boldsymbol{l})$ $\times\theta\sum_{s}\delta^{\kappa}(\boldsymbol{p}_2-\boldsymbol{p}_s+\tfrac{1}{2}\hbar\boldsymbol{k}_2-\hbar\boldsymbol{l})\exp(-\hbar\boldsymbol{l}\boldsymbol{D}_{rs})\exp(\tfrac{1}{2}\hbar\boldsymbol{l}\boldsymbol{D}_{12})$ $+v(l)\theta\sum_{r}\delta^{\kappa}(\boldsymbol{p}_1-\boldsymbol{p}_r+\tfrac{1}{2}\hbar\boldsymbol{k}_1-\hbar\boldsymbol{l})$ $\times[1+\theta\sum_{s}\delta^{\kappa}(\boldsymbol{p}_2-\boldsymbol{p}_s-\tfrac{1}{2}\hbar\boldsymbol{k}_2)]\exp(-\tfrac{1}{2}\hbar\boldsymbol{l}\boldsymbol{D}_{1r})\exp(-\tfrac{1}{2}\hbar\boldsymbol{l}\boldsymbol{D}_{2r})$ $+v(l)\theta\sum_{s}\delta^{\kappa}(\boldsymbol{p}_2-\boldsymbol{p}_s+\tfrac{1}{2}\hbar\boldsymbol{k}_2-\hbar\boldsymbol{l})$ $\times[1+\theta\sum_{r}\delta^{\kappa}(\boldsymbol{p}_1-\boldsymbol{p}_r-\tfrac{1}{2}\hbar\boldsymbol{k}_1)]\exp[-\tfrac{1}{2}\hbar\boldsymbol{l}\boldsymbol{D}_{1s}]\exp[-\tfrac{1}{2}\hbar\boldsymbol{l}\boldsymbol{D}_{2s}]$
$\hat{f}_{1n}$		c	$\langle \boldsymbol{k}_1\|\mathscr{M}_{1n}\|\boldsymbol{k}_n'\rangle = i\hbar^{-1}\Omega^{-1}\,\delta^{\kappa}(\boldsymbol{k}_n'-\boldsymbol{k}_1)[\mathrm{F}(\boldsymbol{k}_1)-\mathrm{F}(-\boldsymbol{k}_1)]$ $\mathrm{F}(\boldsymbol{k}_1) = [v(k_1)+\theta v(\|\boldsymbol{p}_1-\boldsymbol{p}_n+\tfrac{1}{2}\hbar\boldsymbol{k}_1\|/\hbar)]$ $\times[1+\theta\sum_{r}\delta^{\kappa}(\boldsymbol{p}_1-\boldsymbol{p}_r-\tfrac{1}{2}\hbar\boldsymbol{k}_1)]\exp(\tfrac{1}{2}\hbar\boldsymbol{k}_1\boldsymbol{D}_{1n})$
$\hat{g}_{1n}$		c	$\langle \boldsymbol{k}_1\|\mathscr{M}_{1n}\|\boldsymbol{k}_1'\rangle = i\hbar^{-1}\Omega^{-1}\,\delta^{\kappa}(\boldsymbol{k}_1'-\boldsymbol{k}_1)$ $\times\theta\sum_{n}[v(\|\boldsymbol{p}_1-\boldsymbol{p}_n-\tfrac{1}{2}\hbar\boldsymbol{k}_1\|/\hbar)-v(\|\boldsymbol{p}_1-\boldsymbol{p}_n+\tfrac{1}{2}\hbar\boldsymbol{k}_1\|/\hbar)]$
$\hat{h}_{2n}$		c	$\langle \boldsymbol{k}_1,\boldsymbol{k}_2\|\mathscr{M}_{2n}\|\boldsymbol{k}_n',\boldsymbol{k}_2'\rangle = i\hbar^{-1}\Omega^{-1}\,\delta^{\kappa}(\boldsymbol{k}_2'-\boldsymbol{k}_1-\boldsymbol{k}_2-\boldsymbol{l})\,\delta^{\kappa}(\boldsymbol{k}_n'+\boldsymbol{l})$ $\times[G(\boldsymbol{k}_1,\boldsymbol{k}_2,\boldsymbol{l})-G(-\boldsymbol{k}_1,-\boldsymbol{k}_2,-\boldsymbol{l})]$ $G(\boldsymbol{k}_1,\boldsymbol{k}_2,\boldsymbol{l}) = v(l)\theta\,\delta^{\kappa}(\boldsymbol{p}_1-\boldsymbol{p}_2+\tfrac{1}{2}\hbar\boldsymbol{k}_1+\tfrac{1}{2}\hbar\boldsymbol{k}_2+\hbar\boldsymbol{l})$ $\times[1+\theta\sum_{s}\delta^{\kappa}(\boldsymbol{p}_2-\boldsymbol{p}_s-\tfrac{1}{2}\hbar\boldsymbol{k}_2)]\exp(-\tfrac{1}{2}\hbar\boldsymbol{l}\boldsymbol{D}_{2n})$ $\times\exp(-\tfrac{1}{2}\hbar\boldsymbol{k}_1\boldsymbol{D}_{21})$

$\hat{j}_{13}$ 

$$\langle k_1, k_2, k_3|\mathscr{M}_{13}|k_1', k_3'\rangle = i\hbar^{-1}\Omega^{-1}\sum_l \delta^\kappa(k_1' - k_1 - k_2 - l)\,\delta^\kappa(k_3' - k_3 + l)$$
$$\times [\mathrm{J}(k_1, k_2, k_3, l) - \mathrm{J}(-k_1, -k_2, -k_3, -l)]$$
$$\mathrm{J}(k_1, k_2, k_3, l) = v(l)\theta\,\delta^\kappa(p_1 - p_2 - \tfrac{1}{2}\hbar k_1 - \tfrac{1}{2}\hbar k_2 - \hbar l)$$
$$\times [1 + \theta\sum_r \delta^\kappa(p_1 - p_r - \tfrac{1}{2}\hbar k_1)][1 + \theta\sum_s \delta^\kappa(p_3 - p_s - \tfrac{1}{2}\hbar k_3)]$$
$$\times \exp(-\tfrac{1}{2}\hbar k_2 D_{12})\exp(-\tfrac{1}{2}\hbar l D_{13})$$
$$+ v(l)\theta\,\delta^\kappa(p_1 - p_2 - \tfrac{1}{2}\hbar k_1 - \tfrac{1}{2}\hbar k_2 - \hbar l)$$
$$\times [1 + \theta\sum_r \delta^\kappa(p_1 - p_r - \tfrac{1}{2}\hbar k_1)]\theta\sum_s \delta^\kappa(p_3 - p_s + \tfrac{1}{2}\hbar k_3 - \hbar l)$$
$$\times \exp(-\tfrac{1}{2}\hbar k_2 D_{12})\exp(-\tfrac{1}{2}\hbar l D_{1s})\exp(-\tfrac{1}{2}\hbar l D_{3s})$$

$\hat{k}_{13}$ 

$$\langle k_1, k_2, k_3|\mathscr{M}_{13}|k_1'\rangle = i\hbar^{-1}\Omega^{-1}\,\delta^\kappa(k_1' - k_1 - k_2 - k_3)$$
$$\times [\mathrm{K}(k_1, k_2, k_3) - \mathrm{K}(-k_1, -k_2, -k_3)]$$
$$\mathrm{K}(k_1, k_2, k_3) = [v(k_3) + v(|p_1 - p_3 - \tfrac{1}{2}\hbar k_1 - \tfrac{1}{2}\hbar k_3|/\hbar)]$$
$$\times \theta\,\delta^\kappa(p_1 - p_2 - \tfrac{1}{2}\hbar k_1 - \tfrac{1}{2}\hbar k_2 - \hbar k_3)$$
$$\times [1 + \theta\sum_r \delta^\kappa(p_1 - p_r - \tfrac{1}{2}\hbar k_1)][1 + \theta\sum_s \delta^\kappa(p_3 - p_s - \tfrac{1}{2}\hbar k_3)]$$
$$\times \exp(-\tfrac{1}{2}\hbar k_2 D_{12})\exp(-\tfrac{1}{2}\hbar k_3 D_{13})$$

$\hat{l}_{14}$ 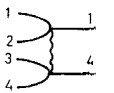

$$\langle k_1, k_2, k_3, k_4|\mathscr{M}_{14}|k_1', k_4'\rangle = i\hbar^{-1}\Omega^{-1}\sum_l \delta^\kappa(k_1' - k_1 - k_2 - l)\delta^\kappa(k_4' - k_3 - k_4 + l)$$
$$\times [\mathrm{L}(k_1, k_2, k_3, k_4, l) - \mathrm{L}(-k_1, -k_2, -k_3, -k_4, -l)]$$
$$\mathrm{L}(k_1, k_2, k_3, k_4, l) = v(l)\theta\,\delta^\kappa(p_1 - p_2 - \tfrac{1}{2}\hbar k_1 - \tfrac{1}{2}\hbar k_2 - \hbar l)$$
$$\times \theta\,\delta^\kappa(p_4 - p_3 - \tfrac{1}{2}\hbar k_3 - \tfrac{1}{2}\hbar k_4 + \hbar l)$$
$$\times [1 + \theta\sum_r \delta^\kappa(p_1 - p_r - \tfrac{1}{2}\hbar k_1)][1 + \theta\sum_s \delta^\kappa(p_4 - p_s - \tfrac{1}{2}\hbar k_4)]$$
$$\times \exp(-\tfrac{1}{2}\hbar k_2 D_{12})\exp(-\tfrac{1}{2}\hbar k_3 D_{43})\exp(-\tfrac{1}{2}\hbar l D_{14})$$

[a] In addition there are vertices obtained by permutation of the numerical indices in $\hat{b}$, $\hat{h}$, $\hat{j}$, $\hat{k}$, and $\hat{l}$.

Table II. Diagrams Corresponding to Table I[a]

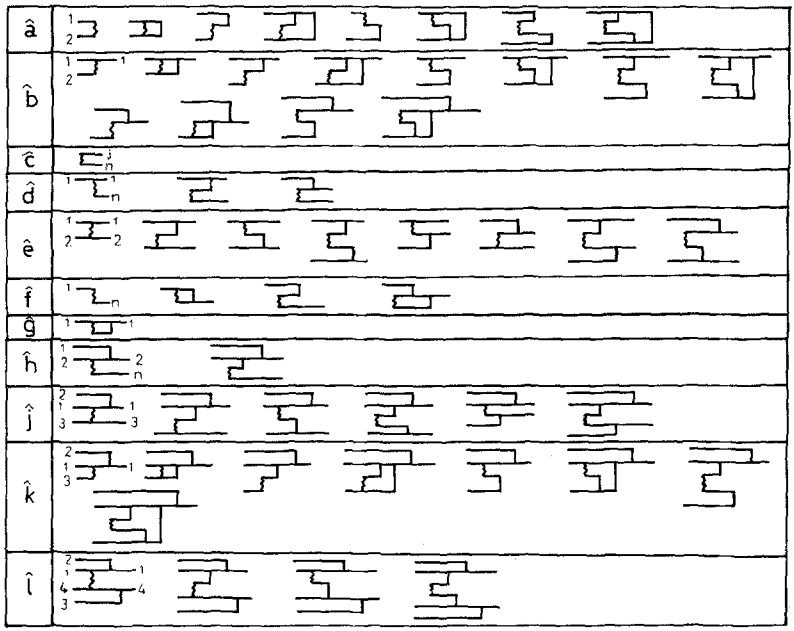

[a] Only diagrams containing the (+) vertex in (10) are shown.

ACKNOWLEDGMENTS

The authors would like to express their thanks to Prof. S. Goto for continuous encouragement and Dr. R. Isizawa for valuable discussions. One of the authors (T.Y.P.) also wishes to express his gratitude to Prof. R. Suzuki for his hospitality.

REFERENCES

1. I. Prigogine and R. Balescu, *Physica* **25**:281 (1959); **25**:302 (1959); **26**:145 (1960); I. Prigogine, *Non-Equilibrium Statistical Mechanics*, Interscience, New York (1962).
2. R. Balescu, *Statistical Mechanics of Charged Particles*, Interscience, New York (1963).
3. L. Van Hove, *Physica* **21**:517 (1955); **23**:441 (1957).
4. N. N. Bogoliubov, *Lectures on Quantum Statistics*, Vol. 1, L. Kline and S. Glass, eds., Gordon and Breach, New York (1967).
5. J. G. Kirkwood, *J. Chem. Phys.* **19**:1173 (1951).
6. I. Prigogine and S. Ono, *Physica* **25**:171 (1959).
7. F. Henin, P. Résibois, and F. Andrews, *J. Math. Phys.* **2**:68 (1961).
8. I. Prigogine, C. George, and F. Henin, *Physica* **45**:418 (1969).
9. R. Balescu, *Physica* **62**:485 (1972).